

Penetrating Spherulitic Growth in Poly(butylene adipate-co-butylene succinate)/Poly(ethylene oxide) Blends

Takayuki Ikehara,* Hironori Kimura, and Zhaobin Qiu†

Department of Applied Chemistry, Faculty of Engineering, Kanagawa University,
3-27-1 Rokkakubashi, Kanagawa-ku, Yokohama 221-8686, Japan

Received February 8, 2005; Revised Manuscript Received April 11, 2005

ABSTRACT: The spherulitic growth of poly(ethylene oxide) (PEO) was found to continue in the spherulites of poly(butylene adipate-co-butylene succinate) (PBAS) in the simultaneous spherulitic growth process of the two components in PBAS/PEO blends. This phenomenon, namely the formation of interpenetrating spherulites (IPS), was analyzed on the basis of birefringence observed by polarizing optical microscopy. The growth direction of PEO lamellae in the PBAS spherulites was found to be along the preexisting PBAS lamellae. PEO crystals also nucleated inside PBAS spherulites and showed spherulitic growth in them at relatively high crystallization temperatures. The conditions for realizing IPS were also discussed. Miscibility in these novel crystalline/crystalline polymer blends in the molten state was confirmed by differential scanning calorimetry and optical microscopy.

Introduction

Investigations of the miscible binary blends of crystalline polymers are still limited compared with those of amorphous/amorphous and crystalline/amorphous polymer blends.^{1–5} When miscible crystalline/crystalline blends are crystallized from a homogeneous melt, the crystallization behavior largely depends on the difference in the melting point T_m of the two components. When the T_m difference is large, the component with higher- T_m crystallizes first, and its spherulites usually fill the whole volume. The lower- T_m component crystallizes at a lower temperature in spatially limited regions inside the spherulites of the other component. When the difference in T_m is small enough, both components have a good possibility to crystallize simultaneously.

The T_m differences in most of the miscible crystalline/crystalline blends reported so far were about 100 °C. In these cases, the two components crystallized at different temperatures as described above. On the other hand, some blends with smaller T_m differences have also been reported.^{6–13} They exhibited simultaneous crystallization of both components.

Moreover, simultaneous spherulitic growth often resulted in the formation of interpenetrating spherulites, i.e., a spherulite of one component continued to grow inside a spherulite of the other component instead of the termination of spherulitic growth when they impinge on each other. Our group have revealed that the penetration of a spherulite take place in poly(butylene succinate)/poly(vinylidene chloride-co-vinyl chloride),^{6–10} poly(butylene succinate-co-butylene carbonate)/poly(L-lactic acid),^{11,12} poly(ethylene succinate)/poly(ethylene oxide),¹³ and poly(3-hydroxybutyrate)/poly(L-lactide) blends.¹⁴

The simultaneous crystallization of both components does not always cause the penetration of lamellae. For instance, linear and branched polyethylene have not been reported to show similar behavior. However, there

is a report on crystalline/amorphous blends that exhibited penetrating lamellae of the same polymer locally around the boundaries of spherulites.¹⁵

This paper reports the miscibility and crystallization behavior of a novel crystalline/crystalline blends of poly(butylene adipate-co-butylene succinate) and poly(ethylene oxide). The T_m difference between the two components is about 31 °C. This leads to a good possibility to realize simultaneous spherulitic growth as well as the penetration of the spherulites. From these points of view, the miscibility and evolution of the morphology in these blends were investigated. The conditions for the formation of interpenetrating spherulites were also discussed.

Experimental Section

Both PEO ($T_m = 67$ °C) and PBAS ($T_m = 98$ °C) were purchased from Aldrich Chemical Co. Solution-cast blends were prepared with mutual solvent chloroform. The samples were first dried at room temperature for 2 days before removing the residual solvent in a vacuum at 50 °C for 2–3 days.

Spherulitic morphology was observed with a polarizing optical microscope (Olympus BH-2) and a temperature controller (Linkam LK-600PM). A first-order retardation plate of 530 nm was used. Thin films of the blends were placed between optical glass plates. They were first melted at about 110 °C and then quenched to a desired crystallization temperature T_c . The crystallization process was recorded in a computer with a CCD camera (Roper Scientific CoolSnap5.0).

The glass transition and melting behavior were analyzed by differential scanning calorimetry (DSC). The weighed samples were sealed in aluminum pans before measurement. They were first melted above the melting point of PBAS, quenched in liquid nitrogen, and then scanned with a DSC instrument (Seiko Instruments DSC6220) in the temperature range from –130 to 130 °C with a scanning rate 10 °C/min under the nitrogen gas flow of 40 cm³/min.

Results and Discussion

Miscibility. Figure 1 shows the DSC thermograms of the glass transition behavior of PBAS/PEO blends. Each sample showed a single glass transition that changed continuously with the blend composition. The blends with the PEO content ϕ_{PEO} of 60 and 80 wt % showed cold crystallization peaks. The step transitions of the samples for $\phi_{\text{PEO}} \geq 80\%$, especially for neat PEO, were small because of the high crystallinity of PEO.

† Present address: College of Materials Science and Engineering, Beijing University of Chemical Technology, Beijing 100029, P. R. China.

* Corresponding author: Tel +81-45-481-5661 ext 3849; Fax +81-45-413-9770; e-mail ikehara@kanagawa-u.ac.jp.

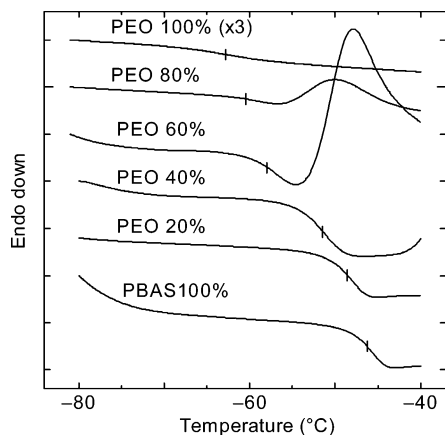


Figure 1. DSC thermograms of the glass transition behavior of PBAS/PEO blends. The data for PEO 100% was tripled in the figure to exhibit clearly its glass transition behavior.

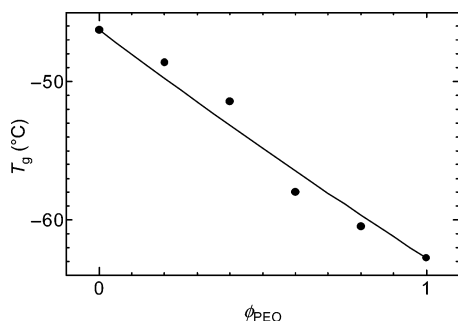


Figure 2. Dependence of the glass transition temperature T_g of PBAS/PEO blends on the PEO content ϕ_{PEO} .

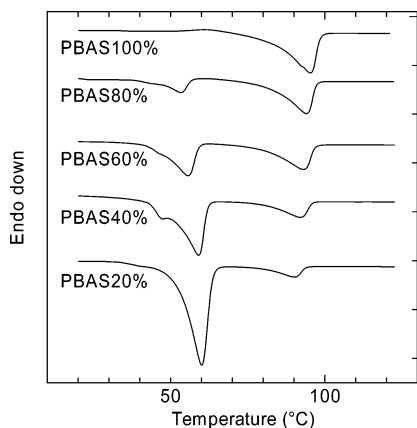


Figure 3. DSC thermograms of the melting behavior of PBAS/PEO blends.

The Fox equation¹⁶ described the composition dependence of the glass transition temperature T_g , as shown in Figure 2. The small discrepancy between the experimental data and the equation can be ascribed to the crystallization in the sample. The crystallization of PEO was inevitable in the quenching process before the T_g measurement. The blend composition in the amorphous region can be different from the original composition. However, the Fox equation approximately described the composition dependence of the apparent values of T_g .

The DSC melting curves are displayed in Figure 3. The lower- and higher-temperature peaks represent the melting of PEO and PBAS, respectively. Both components showed melting point depression, and the peak temperatures are plotted against the blend composition in Figure 4.

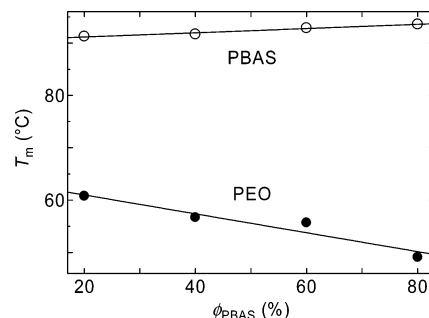


Figure 4. Dependence of the melting peak temperature T_m of PBAS/PEO blends on the PBAS content ϕ_{PBAS} in the blends.

The single T_g and the melting point depression show the miscibility in the PBAS/PEO blends. One-phase melts above the melting points of the two components were confirmed by optical microscopy, too.

Penetrating Growth of Spherulites. Both neat PEO and PBAS spherulites show negative birefringence under crossed polarizers, and only PBAS spherulites show extinction rings. PBAS has smaller birefringence than PEO probably because it is a copolymer and has a low degree of crystallinity. When they are observed by polarizing optical microscopy, the spherulites of the two substances can be easily distinguished based on birefringence, namely brightness, and the presence of the extinction rings. PEO crystals are brighter than those of PBAS in polarizing microscopy because of the difference in birefringence.

The spherulites of both components simultaneously grew in the melt for around $30\% \leq \phi_{PEO} \leq 90\%$ and $46^\circ\text{C} \leq T_c \leq 56^\circ\text{C}$. Figure 5 shows the simultaneous spherulitic growth process of both components in a PBAS/PEO blend. The spherulite with extinction rings and small birefringence is PBAS (top) and the spherulite with large birefringence is PEO (center). The spherulite of PEO impinged on that of PBAS in Figure 5a, and it continued to grow inside the PBAS spherulite in Figure 5b instead of growth termination. The brightness of the PBAS spherulite increased in the region where PEO crystallized. The growth front of the PEO spherulite finally passed through the PBAS spherulite and continued to grow in the melt in Figure 5c. The growth of the PBAS spherulite terminated at this stage.

The penetration of the PEO spherulite into the PBAS spherulite can be proved by the same discussions as in our previous works.^{7,11,13} First, the increase in brightness, namely birefringence, clearly shows that PEO crystallized inside the PBAS spherulite. If the PEO spherulite had developed only outside of the PBAS spherulite and had just engulfed them as in the case of α - and β -forms of isotactic polypropylene, the brightness of the PBAS spherulite would have been constant.

Second, the change in birefringence inside the PBAS spherulite shows that the PEO lamellae grow along the PBAS lamellae instead of forming a layered structure where one spherulite is placed on the other. In the case of the layered structure, the lamellae of PEO would grow in the radial direction of the PEO spherulite even inside the region of the PBAS spherulite. In the present case, however, Figure 5b shows no PEO lamellae that grew in the radial direction inside the PBAS spherulite, which is evidenced by the additive birefringence (orange color) in the third quadrant (the lower left quarter) of the PBAS spherulite. The apparent birefringence here would be subtractive birefringence (blue color) in the

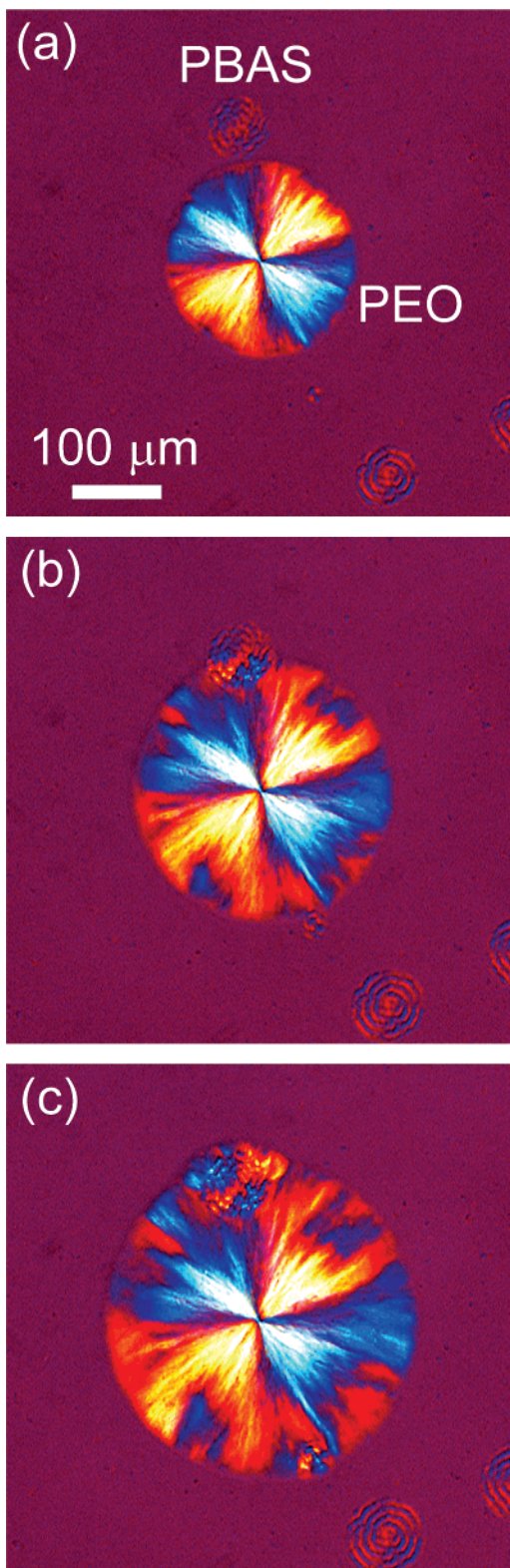


Figure 5. Penetration process of a PEO spherulite into a PBAS spherulite in the blend of PBAS/PEO = 3/7 crystallized at 48 °C. Crystallization times were (a) 27, (b) 35, and (c) 44 s.

case of a layered structure since the left half of the PBAS spherulite is located in the second quadrant of the PEO spherulite and since the birefringence of PEO is larger than that of PBAS. These results indicate that the PEO lamellae grew along the PBAS lamellae without forming a layered structure, i.e., the PEO spherulite penetrated into the PBAS spherulite in the

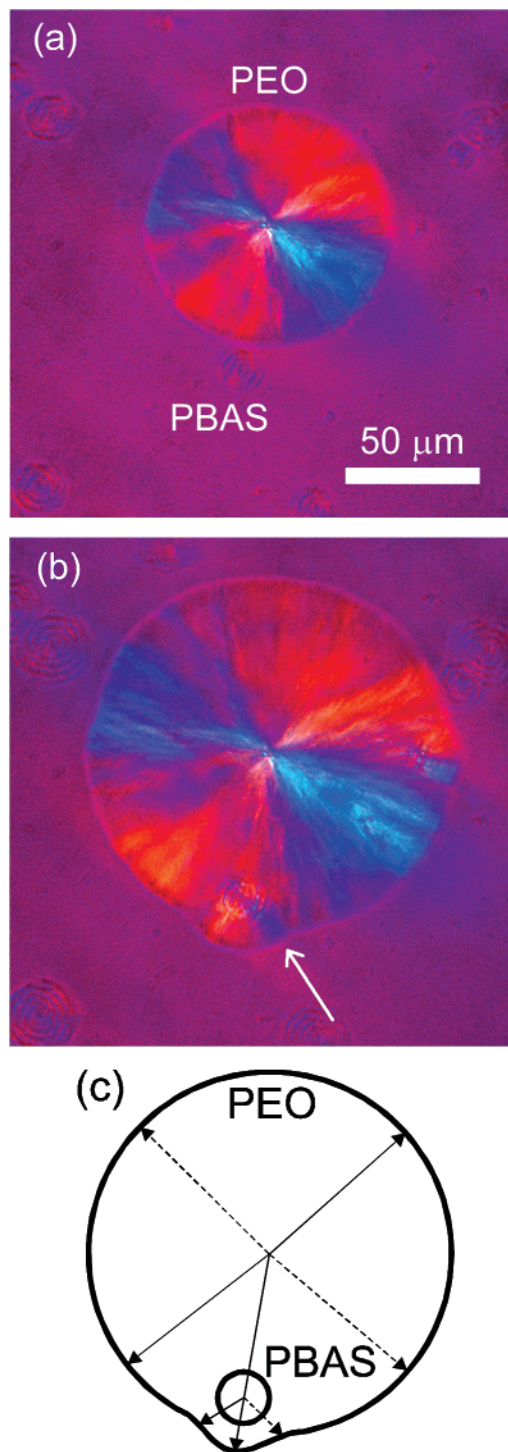


Figure 6. Polarized optical micrographs of the blend of PBAS/PEO = 2/8 crystallized at 50 °C that show the growth of PEO lamellae along the PBAS lamellae as indicated by the arrow. Crystallization times were (a) 95 and (b) 122 s. (c) The schematic figure of (b). The solid and dashed arrows indicate the lamellar growth directions of additive and subtractive birefringence, respectively.

crystallization process. Finally, the characteristic size of the lateral structure is much larger than the thickness of the sample (about 1 μm).

Figure 6 shows another evidence for the growth of PEO lamellae along PBAS lamellae. Here, the spherulite with extinction rings and smaller birefringence on the lower left side is PBAS and the spherulite with larger birefringence at the center is PEO. The PEO spherulite contacted with the PBAS spherulite in Figure

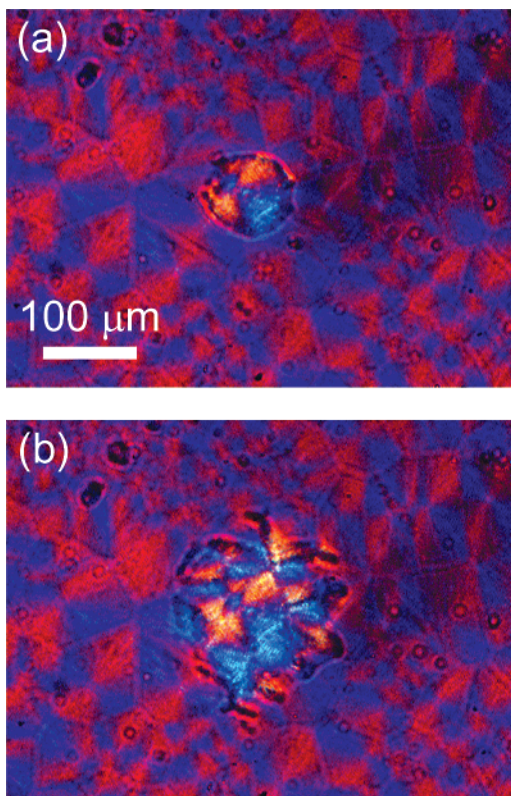


Figure 7. Nucleation and spherulitic growth of PEO in PBAS spherulites after PBAS spherulites had filled the whole sample. PBAS/PEO = 4/6 and $T_c = 56^\circ\text{C}$. Crystallization times were (a) 19 and (b) 39 min.

6a. After the penetrating growth of PEO spherulite into the PBAS spherulite, a part of the PEO spherulite in its third quadrant showed subtractive birefringence, as indicated by the arrow in Figure 6b. It must have been caused by the PEO lamellae that grew along the PBAS lamellae in the fourth quadrant of the PBAS spherulite and continuously developed in the melt with their growth direction unchanged (Figure 6c). The negative spherulite of PEO usually causes additive birefringence in the first and third quadrants of the spherulites and subtractive birefringence in the second and fourth quadrants with the use of a first-order retardation plate.

The spherulitic growth rate of PEO is obviously faster in the PBAS spherulite, as shown in Figure 6b. The growth front of PEO that passed through the PBAS spherulite preceded the other portion of the growth front. This can be ascribed to the rejected PEO amorphous chains from the PBAS crystals into the interlamellar regions in the PBAS spherulite. The concentration of PEO is therefore higher than the overall PEO content in the interlamellar region of PBAS.

PEO nucleated in PBAS spherulites at higher T_c as shown in Figure 7 after they had filled the whole sample. It continued to grow inside the PBAS spherulites keeping the spherulitic shape. The spherulitic growth of PEO continued until it contacted with another PEO spherulite, and PEO spherulites eventually filled the whole sample, too. This type of nucleation and spherulitic growth was also found in poly(butylene succinate)/poly(vinylidene chloride-co-vinyl chloride) blends,¹⁰ poly(butylene succinate-co-butylene carbonate)/poly(L-lactic acid) blends,¹¹ poly(butylene succinate)/poly(ethylene oxide) blends,¹⁷ and poly(vinylidene fluoride)/poly(3-hydroxybutyrate-co-hydroxyvalerate) blends.¹⁸

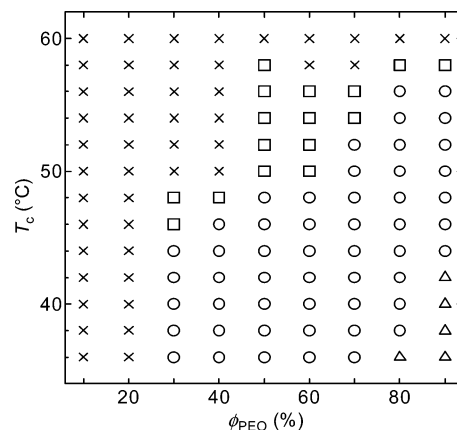


Figure 8. Dependence of the spherulitic behavior in PBAS/PEO blends on the crystallization temperature T_c and the PEO content ϕ_{PEO} : cross, only PBAS crystallized; triangle, only PEO crystallized; square, PBAS spherulites first filled the whole sample before the nucleation of PEO inside the PBAS spherulites; circle, simultaneous crystallization and penetration of spherulites took place.

The brightness of the PBAS spherulites increased in the same way as in the simultaneous spherulitic growth of Figures 5 and 6.

The spherulitic growth behavior is summarized in Figure 8. Only PBAS nucleated for $\phi_{\text{PEO}} \leq 20\%$. Only PEO nucleated at lower T_c for $\phi_{\text{PEO}} \geq 80\%$. Both components nucleated in the intermediate compositions and T_c . Under these conditions, the simultaneous spherulitic growth occurred in the relatively lower T_c . The nucleation and growth of PEO spherulites inside PBAS spherulites occurred relatively in the higher temperature region. This behavior can be ascribed to the difference in T_m of the two constituents. At relatively high T_c , the smaller degree of supercooling for PEO, the lower- T_m component, causes its slower nucleation rate.

Conditions for Penetration of Spherulites. Penetration of spherulites described above requires several conditions. First, the difference in T_m of the two constituents must be sufficiently small when both components crystallize simultaneously. It is 31°C for the present blend system. The T_m differences are generally less than about 35°C in the blends where both components develop spherulites simultaneously.⁶⁻¹³

Second, the content of the higher- T_m component should be smaller than that of the lower- T_m component to realize the simultaneous development of the spherulites of both components. When a blend sample is isothermally crystallized, the degree of supercooling of the higher- T_m component is larger than that of the lower- T_m component even if the melting point depression is taken into account. Figure 8 actually shows that the simultaneous spherulitic growth takes place mainly for $\phi_{\text{PEO}} \geq 50\%$. In the present system, PEO is the component with lower T_m .

Third, the spherulites of penetrated component must contain a sufficient amount of interlamellar amorphous regions that contain an adequate quantity of the penetrating component. The asymmetry in the composition described above realizes this situation since no interspherulitic amorphous regions are formed in the crystalline/crystalline blends investigated so far. The penetrating spherulites crystallize in these large interlamellar regions. The model of the spherulites that are sparse or dense with crystalline lamellae is described elsewhere in more detail.⁷

Conclusions

Melting point depression, single glass transition, and the observation by optical microscopy showed the miscibility of the blends of PBAS and PEO. Both components simultaneously developed spherulites for $\phi_{\text{PEO}} \geq 20\%$ at most of the crystallization temperatures in the present paper. PEO spherulites continued its growth inside PBAS spherulites after they impinged on each other, and they formed interpenetrating spherulites. The analysis based on birefringence showed that the lamellae of PEO developed along those of PBAS. This can explain the change in birefringence in the PBAS spherulite after the crystallization of PEO. These blends therefore formed interpenetrating spherulites, where the lamellae of both components are interlocked by each other. PEO also nucleated and grew inside the PBAS spherulites at relatively high T_c . The penetration of PEO spherulites can be mainly ascribed to the PBAS spherulites sparse with lamellae. They contain an adequate quantity of uncrystallized PEO. The spherulitic growth rate of PEO was faster in PBAS spherulites than in the melt. The quantitative analysis of the growth rate will be published in the near future.

References and Notes

- (1) Avella, M.; Martuscelli, E. *Polymer* **1988**, *29*, 1371.
- (2) Cheung, Y. S.; Stein, R. S. *Macromolecules* **1994**, *27*, 2512.
- (3) Penning, J. P.; Manley, R. S. J. *Macromolecules* **1996**, *29*, 77.
- (4) Liu, A. S.; Liau, W. B.; Chiu, W. Y. *Macromolecules* **1998**, *31*, 6539.
- (5) Lee, J. C.; Tazawa, H.; Ikehara, T.; Nishi, T. *Polym. J.* **1998**, *30*, 327.
- (6) Lee, J. C.; Tazawa, H.; Ikehara, T.; Nishi, T. *Polym. J.* **1998**, *30*, 780.
- (7) Ikehara, T.; Nishi, T. *Polym. J.* **2000**, *32*, 683.
- (8) Terada, Y.; Ikehara, T.; Nishi, T. *Polym. J.* **2000**, *32*, 900.
- (9) Hirano, S. Y.; Terada, Y.; Ikehara, T.; Nishi, T. *Polym. J.* **2001**, *33*, 2001.
- (10) Terada, Y.; Hirano, S.; Ikehara, T.; Nishi, T. *Macromol. Symp.* **2001**, *175*, 209.
- (11) Hirano, S.; Nishikawa, Y.; Terada, Y.; Ikehara, T.; Nishi, T. *Polym. J.* **2002**, *34*, 85.
- (12) Ikehara, T.; Nishikawa, Y.; Nishi, T. *Polymer* **2003**, *44*, 6657.
- (13) Qiu, Z.; Ikehara, T.; Nishi, T. *Macromolecules* **2002**, *35*, 8251.
- (14) Blümm, E.; Owen, A. J. *Polymer* **1995**, *36*, 4077.
- (15) Gałęski, A.; Grębowicz, J.; Kryszewski, M. *Makromol. Chem.* **1983**, *184*, 1323.
- (16) Fox, T. G. *Bull. Am. Phys. Soc.* **1956**, *1*, 123.
- (17) Qiu, Z.; Ikehara, T.; Nishi, T. *Polymer* **2003**, *44*, 2799.
- (18) Qiu, Z.; Fujinami, S.; Komura, M.; Nakajima, K.; Ikehara, T.; Nishi, T. *Polymer* **2004**, *45*, 4355.

MA0502809